

Deep neural network for optimal retirement consumption in defined contribution pension system

Wen Chen^{1,2} and Nicolas Langrené¹

¹Commonwealth Scientific and Industrial Research Organisation, Data61, RiskLab Australia

²Corresponding author. Email: wen.chen@csiro.au

December 22, 2024

Abstract

In this paper, we develop a deep neural network approach to solve a lifetime expected mortality-weighted utility-based model for optimal consumption in the decumulation phase of a defined contribution pension system. We formulate this problem as a multi-period finite-horizon stochastic control problem and train a deep neural network policy representing consumption decisions. The optimal consumption policy is determined by personal information about the retiree such as age, wealth, risk aversion and bequest motive, as well as a series of economic and financial variables including inflation rates and asset returns jointly simulated from a proposed seven-factor economic scenario generator calibrated from market data. We use the Australian pension system as an example, with consideration of the government-funded means-tested Age Pension and other practical aspects such as fund management fees. The key findings from our numerical tests are as follows. First, our deep neural network optimal consumption policy, which adapts to changes in market conditions, outperforms deterministic drawdown rules proposed in the literature. Moreover, the out-of-sample outperformance ratios increase as the number of training iterations increases, eventually reaching outperformance on all testing scenarios after less than 10 minutes of training. Second, a sensitivity analysis is performed to reveal how risk aversion and bequest motives change the consumption over a retiree's lifetime under this utility framework. Our results show that stronger risk aversion generates a flatter consumption pattern; however, there is not much difference in consumption with or without bequest until age 103. Third, we provide the optimal consumption rate with different starting wealth balances. We observe that optimal consumption rates are not proportional to initial wealth due to the Age Pension payment. Forth, with the same initial wealth balance and utility parameter settings, the optimal consumption level is different between males and females due to gender differences in mortality. Specifically, the optimal consumption level is slightly lower for females until age 84.

Keywords: decumulation, retirement income, deep neural network, stochastic control, economic scenario generator, defined-contribution pension, optimal consumption

JEL Classification: C45, D81, E21, C53

MSC Classification: 91G60, 62P05, 62M45, 93E20, 91B70, 65C05, 91B16

1 Introduction

The global trend of transition from defined benefit (DB) to defined contribution (DC) system means that responsibility switched from employers to employees, making life-cycle management an important and relevant topic to every individuals. In Australia, the DC system established in 1992, requires employers to contribute a minimum percentage (Superannuation Guarantee rate^{*}) of employee's earnings to a superannuation fund. Over 28 years, the Australia DC system has reached a mature stage, and achieved retirement savings of

^{*}The SG rate was 9.5% on 1 July 2014, and will remain 9.5% rate until 30 June 2021, and is set to have five annual increases, where the SG rate will increase to 12% by July 2025.

around \$3 trillion (AUD) in asset, and has the highest proportion in DC assets (86%) relative to DB assets (14%) (Towers Watson, 2020). More new retirees now own significant superannuation savings accumulated during their working lives. However, there is little guidance on how to achieve the best strategies after retirement. Also due to reasons such as fear of ruin and bequest motive, most retirees tend to only withdraw the statutory minimum rate from their retirement account (Sneddon et al. 2016, De Ravin et al. 2019), thus not optimising benefit from their retirement savings. Designing income solution becomes a major challenge for the Australian superannuation fund industry. The retirement income solution in the decumulation phase is underdeveloped. In the academic as well as the industrial practitioner literature, the utility framework has been used to analyse complex life-cycle management problems which involve consumption, asset allocation and possibly other decisions. The utility function reduces the dimension of the problem by providing a quantitative measure of uncertain retirement outcome satisfaction resulting from different deterministic or dynamic financial strategies, such as drawdown strategies and investment strategies. Since the seminal contribution of Yaari (1964, 1965) on utility based life-cycle models in asset allocation and optimal consumption, alternative methods and extensions have been investigated.

For example, Thorp et al. (2007) investigated optimal investment and annuitisation strategies for the decumulation phase using a Hyperbolic Absolute Risk Aversion (HARA) utility function. Huang et al. (2012) proposed a partial differential equation (PDE) framework for optimal consumption with stochastic force of mortality and deterministic investment returns to maximise discounted expected Constant Relative Risk Aversion (CRRA) utility over a random time horizon. Mao et al. (2014) also looked at the optimal consumption problem during decumulation, in conjunction with related decision problems such as optimal retirement age and optimal leisure time, using CRRA utility. Ding et al. (2014) used a CRRA utility, focusing on optimal portfolio allocation and the effect of bequest. Andréasson et al. (2017) investigated the optimal consumption, investment and housing decisions with means-tested public pension in retirement, using a HARA utility function discounted by inflation. Butt et al. (2018) considered the optimal consumption and asset allocation problems with Age Pension taken into account, using CRRA utility. De Ravin et al. (2019) designed a mortality weighted CRRA utility-based metric called the Members Default Utility Function (MDUF) to assist industry to design retirement outcome solutions for the decumulation phase. Finally, a recent attempt to avoid the expected utility approach is Forsyth et al. (2019), in which a CVaR approach is used to manage depletion risk via asset allocation throughout both the accumulation and decumulation phases in a DC system.

In practice, the most popular approach for solving such optimal decumulation stochastic control problems is numerical dynamic programming with state discretisation and interpolation (Rust 1996, Andréasson et al. 2017, Butt et al. 2018, De Ravin et al. (2019), Jin et al. 2020). Other popular approaches include analytical or semi-analytical solutions (Yaari 1965, Ding et al. 2014) and numerical schemes for Hamilton-Jacobi-Bellman (HJB) PDE (Cairns et al. 2006, Huang et al. 2012, Forsyth et al. 2019).

The analytical solution approach is the most attractive, but is unfortunately usually infeasible or requires too significant simplifications of the original problem to remain useful in practice. The numerical dynamic programming and PDE approaches are able to solve more realistic problem with a greater set of features, but both suffer from the curse of dimensionality, which puts a limit on the number of stochastic factors which can be accounted for.

In order to break the limitations of these classical numerical approaches, we propose in this paper a deep neural network approach (DNNs, Goodfellow et al. 2016). The principle is to model the unknown consumption policy by a DNN and to optimize it directly by modern gradient descent techniques. This bypasses the dynamic programming principle altogether, overcomes the curse of dimensionality (Poggio et al. 2017, Han et al. 2018), and makes it possible to consider as many realistic features and stochastic factors as deemed necessary to obtain informative consumption advice in the decumulation phase in a DC system. Being able to account for a great range of customized features and personal objectives in the decision-making process with machine learning technology shall improve member engagement in the DC system (Fry, 2019).

Approximating policies by DNNs have been well explored in the reinforcement learning field, see Sutton and Barto (2018, Chapter 13), with great practical success as illustrated for example by the famous AlphaGo and AlphaGo Zero programs Sutton and Barto (2018, Chapter 16). For the most part, reinforcement learning is concerned with infinite time horizon problems, coupled with discrete-valued control spaces. By contrast, this paper addresses a finite time horizon stochastic control problem (due to mortality) with continuous policies

(namely consumption). In this context, optimal policies should explicitly depend on time, either time since inception t or time to maturity $T - t$, where T is the maturity.

Classically, the optimal policies of stochastic control problems with finite time horizon are estimated in a backward manner, taking advantage of the dynamic programming principle (Beckmann, 1968). Recently, DNNs have been used in this context in Huré et al. (2018), Bachouch et al. (2018) and Fécamp et al. (2019) for approximating value functions, policy functions or both. As an alternative to the classical backward dynamic programming approach, Han and E (2016) suggested to use one DNN policy function for each decision time t_i , yielding a collection of sub-networks, indexed by time, and trained simultaneously. This global policy learning approach has been used in Fécamp et al. (2019) for financial option hedging problems, in Guo et al. (2019) for robust portfolio allocation, and has been adapted to optimal stopping problems in Becker et al. (2019) with application to exotic option pricing.

One modification of this global approach is to consider one single DNN and include time as part of the inputs, in addition to all the other state variables. The very same DNN can then be used at all decision times. Fécamp et al. (2019) also implemented and tested this modification, and Li and Forsyth (2019) used it for an asset allocation problem. This single DNN approach can be thought of as the adaptation of recurrent neural networks (RNN) to finite-horizon problems, for which policies do change over time and therefore time needs to be part of the inputs of this single DNN. As such a modification is much more parsimonious, easier to train and better suited to problems for which policies vary in a smooth manner over time, we make use of this approach in this paper to model and learn optimal consumption policies.

The main contribution of this paper is the proposed use of a DNN-policy approach to realistic utility maximisation problems driven by multi-factor economic stochastic model. Our approach is very general: as it does not rely on dynamic programming, the objective function is not limited to expected utility and is allowed to be more sophisticated and personalised; as it is simulation-based, all the realistic features of the problem, such as fees and Age Pension policy can be easily accounted for; finally, the ability of DNNs to handle large-scale problems means that the economic scenario generator (ESG) used to represent the state of the economy can contain as many stochastic variables as deemed necessary. The second contribution of this paper is a proposed 7-factor ESG which we use to perform numerical experiments and obtain findings on realistic decumulation test cases in the Australian DC pension system.

The paper is organized as follows. Section 2 formulates the problem and introduces useful notations. Section 2.2 introduces the ESG used for our numerical tests. Section 3 details the DNN numerical approach used to solve our utility maximization problem. Section 4 presents our numerical results on several test cases based on the Australian superannuation system. Finally, Section 5 concludes the paper and suggests several areas of future work.

2 Problem formulation

In this section, we introduce our utility-based objective function (subsection 2.1), a stochastic economic model in the form of an Economic Scenario Generator (ESG, subsection 2.2) which provides us with Monte Carlo simulations of economic variables, means-tested Age Pension (subsection 2.3) and wealth dynamics (subsection 2.4).

2.1 Objective function

The objective of this problem is to maximise the mortality-weighted expected utility through a dynamic consumption policy in order to obtain the optimal consumption level in the future under any market conditions. We formulate the objective function similar to the MDUF proposed in Bell (2017); De Ravin et al. (2019), with the wealth of the retiree following the dynamics defined in subsection 2.4.

When entering retirement at time $t = 0$, the total utility of one single person is defined as follows.

$$V_0(w_0) = \max_{\{c_t\}_{0 \leq t \leq T}} \mathbb{E} \left[\sum_{t=0}^T \{ {}_t p_x u(c_t) + {}_{t-1} q_x v(w_t) \} \right] \quad (2.1)$$

subject to

$$c_t \in [0, w_t + a_t] \quad (2.2)$$

where x is the retirement age (in years) which is set to be 67, and the maximum age is set to be 108, therefore the time horizon is $T = 41$. c_t is the annual consumption, w_t is the wealth and a_t is the Age Pension payment subjected to means test at decision time t , where $t = 0, 1, \dots, T$. All these three variables are expressed in real terms, adjusted for inflation, when computing the utilities. The consumption c_t should be positive and less than the total wealth plus the Age Pension payment at any time t . The consumption utility function $u(c_t)$ is a CRRA type with consumption risk aversion parameter ρ ($\rho = 0$ being risk neutral) defined as

$$u(c_t) = \frac{c_t^{1-\rho}}{1-\rho}, \quad (2.3)$$

and the final utility of the residual wealth $v(w_t)$ if the person dies between $t - 1$ and t is defined as

$$v(w_t) = \frac{w_t^{1-\rho}}{1-\rho} \left(\frac{\phi}{1-\phi} \right)^\rho, \quad (2.4)$$

with strength of bequest motive $\phi \in [0, 1)$. The higher ϕ , the stronger the bequest motive. Conversely, $\phi = 0$ means there is no desire to leave wealth unspent after death.

${}_t p_x$ is the probability of surviving at age $x + t$ conditional on being alive at age x . It can approximate the state of health. ${}_{t-1|q_x}$ is the probability of death during $(x + t - 1, x + t]$ conditional on being alive at age x . We assume that the male and female retirees are subject to the mortality rates in Australian Life Tables 2015-17 published by Australian Government Actuary (AGA, [Australian Government Actuary 2017](#)). Since the problem involves ageing and the time span covers several decades, it is important to allow for future improvements in mortality rates. We assume the mortality rates decrease with the 25-year improvement factor as published by the AGA, to project the mortality rates that could be expected to occur over an individual's lifetime*. We also assume that mortality rates are independent of retirement wealth, consumption and portfolio returns.

2.2 Economic scenario generator

To complete the definition of the utility maximization problem (2.1), we need a model to describe economic variables such as inflation and the asset returns which affect the wealth of the retiree as well as its age pension entitlements. In [Bell \(2017\)](#); [De Ravin et al. \(2019\)](#), the authors used a fixed risk-free rate and assume the returns of the risky asset follow a normal distribution. Such constant or fixed investment return distribution assumptions are common and convenient for computational reasons, but can be deemed too basic to properly capture uncertainties inherent in the financial market for retirement management. In the present work, one convenient consequence of the proposed deep learning approach for solving (2.1) (Section 3) is that the specific choice of model for the economic variables of the problem does not restrict the numerical feasibility of the utility maximization problem (2.1).

In this paper, we propose to use a multivariate stochastic investment model in the form of an Economic Scenario Generator (ESG, [Moudiki and Planchet 2016](#)), which are commonly applied in the actuarial field to simulate future economic and financial variables. A well-known ESG is Wilkie's four-factor investment model ([Wilkie, 1984](#)) which models inflation rates, equity returns and bond returns as stochastic time series through a cascading structure to describe the investment returns. A series of updates and extensions of this model have been proposed on both practical and theoretical aspects ([Wilkie, 1995](#); [Şahin et al., 2008](#); [Wilkie and Şahin, 2017, 2019](#)). The Ahlgrim model ([Ahlgrim et al., 2005](#)) developed for the Casualty Actuarial Society extends the model to include real estate prices. [Zhang et al. \(2018\)](#) revisit Wilkie's model and examine the model performance for the United States. Based on the model in [Wilkie \(1995\)](#), [Butt and Deng \(2012\)](#) propose an ESG model to investigate investment strategies for the Australian DC pension system. [Chen et al. \(2020a\)](#) extended the SUPA model of [Sneddon et al. \(2016\)](#) to a 14-factor SUPA model for the Australian system, and use it to quantify uncertainty and model downside risks with retirement savings in the accumulation and decumulation phases.

*The details on how to use life tables and the mathematical form of incorporating future improvements can be found at: http://aga.gov.au/publications/life_table_2010-12/07-Part3.asp

2.2.1 Seven-factor economic scenario generator

We design a seven-factor ESG covering inflation and six asset classes, which is sufficient for completing the description of the optimal decumulation problem (2.1).

Our ESG models the dynamics of inflation $q(t)$, risky asset returns such as domestic and international total equity returns $e(t)$ and $n(t)$, real estate returns $h(t)$, and defensive asset returns such as interest rates $s(t)$ and domestic and international bond returns $b(t)$ and $o(t)$. Similar to Wilkie’s model (Wilkie, 1984), we assume the inflation rate $q(t)$ follows a discretised mean-reverting Ornstein-Uhlenbeck process (a.k.a. AR(1) process). From there, the specific dynamics of each economic factor and their dependence are summarized in Table A.2 in Appendix A. The model is calibrated to historical data from year 1992 when the Superannuation Guarantee started, to year 2020. The data are obtained from the Reserve Bank of Australia (RBA), Australian Bureau of Statistics (ABS) and Bloomberg. Table A.2 also reports the calibrated values on the considered dataset.

The simulated inflation allows us to project the future Age Pension rates and the mean-test thresholds values, so we can compute the future Age Pension eligible payment under the current pension policy. We also use inflation-adjusted consumption and wealth to compute their utilities. The simulated asset returns allow us to compute the returns of the predefined portfolios described in the next subsection 2.2.2.

2.2.2 Simulation of portfolio returns

We build investment portfolios across the aforementioned six different asset classes. According to the Government website MoneySmart, there are four common types of life-cycle investment strategies: *Cash*, *Conservative*, *Balanced* and *Growth* with 0%, 30%, 70% and 85% invested in growth assets respectively. In this paper, we adopt the portfolios settings in Chen et al. (2020b) where the growth (risky) assets include 50% Australian equity (domestic) $e(t)$, 30% international equity (excluding Australia) $n(t)$ and 20% property $h(t)$, and the defensive assets include 30% risk-free term deposit $s(t)$, 50% domestic bond $b(t)$ and 20% international bond $o(t)$ [†]. Then the returns of the growth and defensive assets are given as follows:

$$\begin{aligned} R_{\text{growth}}(t) &= 50\%e(t) + 30\%n(t) + 20\%h(t), \\ R_{\text{defensive}}(t) &= 0\%s(t) + 50\%b(t) + 20\%o(t). \end{aligned}$$

In our numerical examples, we select the *Balanced* investment strategy, with $\omega = 70\%$ invested in growth assets and 30% invested in defensive assets.

$$R(t) = \omega \cdot R_{\text{growth}}(t) + (1 - \omega) R_{\text{defensive}}(t). \quad (2.5)$$

We keep these weights fixed throughout retirement.

2.3 Age Pension simulation

The Age Pension is a government payment scheme which provides income to help Australian retirees to cover their cost of living. It is paid to people who meet the retirement age requirement, subject to an income test and an asset test. The payment rates also depend on the family (single or couple) and home-ownership status. The pension age in 2020 is 66 and will be gradually increased to 67 by 2023. The payment rates and the thresholds are adjusted by changes in Consumer Price Index (CPI) or the Pensioner and Beneficiary Living Cost Index twice a year[‡].

In the following, we consider a 67-year-old single homeowner who converted all liquid assets into the account-based pension and has no other income stream. We assume the payment rates and test thresholds are only adjusted for inflation rates annually. Based on these assumptions, the payment is determined by the wealth, deemed income from the liquid assets, and the compound inflation

$$Q_t = e^{\sum_{s=0}^t q_s}. \quad (2.6)$$

[†]These weights reflect a lower exposure to both growth assets (50% v 66%) and international assets (25% v 36%) on the average Australian Prudential Regulation Authority (APRA) regulated superannuation fund asset allocations as at December 2019, reflecting the conservative nature of typical retiree allocations. More information is available at: <https://www.apra.gov.au/quarterly-superannuation-statistics> (Retrieved June 4, 2020).

[‡]More details about Age Pension can be found at: <https://www.dss.gov.au/seniors/benefits-payments/age-pension>

The Age Pension A_t this person can receive at time t is the minimum of the payment under the asset test A_t^A and income test A_t^I , that is $A_t(W_t, Q_t) = \min(A_t^A, A_t^I)$ where

$$A_t^A = \max(A_t^{\max} - \tau^A \max[(W_t - W_t^A), 0])$$

$$A_t^I = \max(A_t^{\max} - \tau^I \max[r_1 \min(W_t, W_t^I) + r_2 \max(W_t - W_t^I, 0) - I_t, 0], 0).$$

A_t^{\max} is the maximum Age Pension, W_t^A is the asset test threshold for full pension, I_t is the income test cutoff point. W_t^I is the lower deeming asset threshold at time t . These four variables are adjusted for inflation with $x_t = x_0 Q_t$ for $x \in [A_t^{\max}, W_t^A, W_t^I, I]$ and $t \in [0, T]$. τ^A and τ^I are the taper rates for asset and income test; r_1 and r_2 are the lower and higher deeming rates; $r_1 < r_2$. These four rates are determined by the Age Pension policy, therefore they are assumed to be constants in this paper.

2.4 Dynamics of wealth

In our model, the wealth is an endogenous stochastic variables which is determined by the market changes and the consumption decisions. The wealth at time $t + 1$ is given as follows:

$$W_{t+1} = (W_t + A_t(W_t, Q_t) - C_t) e^{R_t} \quad (2.7)$$

where W_t , A_t and C_t are the future (non-deflated) value of wealth, Age Pension, and consumption. $w_t = W_t/Q_t$, $a_t(W_t, Q_t) = A_t(W_t, Q_t)/Q_t$ and $c_t = C_t/Q_t$ are the wealth, Age Pension and consumption in real terms. Note that the consumption consists of the drawdown from the wealth plus the Age Pension payment. When evaluating the utility of the future consumption and residual wealth, we used consumption and wealth in real terms.

3 Numerical method

Now that the problem has been fully described in detail, this section focuses on the numerical method and solution.

3.1 Empirical objective function

Problem (2.1) is a discrete-time finite horizon stochastic control problem. Its optimal policy (consumption) is affected in feedback form by the stochastic state variables of the economic scenario generator described in Subsection 2.2 and by the wealth (Subsection 2.4).

More specifically, the state variables of Problem (2.1) are the wealth W (Eq (2.7)), the investment return R (Eq (2.5)) and the compound inflation discount factor Q (Eq (2.6)).

We use a parametric consumption policy approach, meaning that we model the set of possible policies by a class of functions $(t, x) \in \mathbb{R}^{d+1} \rightarrow c(t, x; \beta)$ indexed by a parameter $\beta \in \mathbb{R}^p$. For a fixed parameter β , the dynamics of the controlled state process $X^c = (W_t, R_t, Q_t)$, valued in \mathbb{R}^3 , is

$$\begin{aligned} X_0^c &= x_0 = (W_0, R_0, Q_0) \\ X_{t+1}^c &= \mathcal{T}(X_t^c, c_t(t, X_t^c; \beta), \epsilon_{t+1}), t = 0, \dots, T-1 \end{aligned}$$

where (ϵ_t) is a sequence of i.i.d. random variables, $c = c_t(t, X_t^c; \beta)$ is the consumption policy and \mathcal{T} is a known transition function given by equations (2.7)-(2.5)-(2.6) and the ESG dynamics in Table A.2.

In practice, we use Monte Carlo simulations to estimate the expectation involved in the objective function (2.1). Let M be the number of Monte Carlo simulations. For each $m = 1, 2, \dots, M$, we compute a simulation path

$$\begin{aligned} X_0^{c,m} &= x_0 = (W_0, R_0, Q_0) \\ X_{t+1}^{c,m} &= \mathcal{T}(X_t^{c,m}, c_t(t, X_t^{c,m}; \beta), \epsilon_{t+1}^m), t = 0, \dots, T-1 \end{aligned}$$

where ϵ_t^m , $m = 1, 2, \dots, M$, are i.i.d. realizations of the random variable ϵ_t . The counterpart of problem (2.1) with sample averaging and parametric control is given by

$$\hat{V}_0^M = \max_{\beta \in \mathbb{R}^p} \frac{1}{M} \sum_{m=1}^M \left[\sum_{t=0}^T \{ {}_t p_x u(c_t(t, X_t^{c,m}; \beta)) + {}_{t-1} q_x v(w_t^{c,m}) \} \right] \quad (3.1)$$

3.2 Deep neural network consumption policy

In order to solve the empirical problem (3.1) in practice, we still need to choose a specific class of parametric functions $(t, x) \in \mathbb{R}^{d+1} \rightarrow c(t, x; \beta)$ to model the consumption policy. We choose to model the control policy by a deep neural network (DNN, Goodfellow et al. 2016). In other words, we consider functions c defined as a composition of linear combinations and nonlinear activation functions:

$$c(t, W, R, Q; \beta) = (W + A_t(W, Q)) \times \mathcal{S}_{\text{out}} \left(b^{(3)} + \sum_{k=1}^{K_3} w_k^{(3)} \varphi_k^{(2)} \right) \quad (3.2)$$

$$\varphi_k^{(2)} = \mathcal{S}_2 \left(b_k^{(2)} + \sum_{k_2=1}^{K_2} w_{k_2,k}^{(2)} \varphi_{k_2}^{(1)} \right), \quad k = 1, 2, \dots, K_3 \quad (3.3)$$

$$\varphi_k^{(1)} = \mathcal{S}_1 \left(b_k^{(1)} + \sum_{k_1=1}^{K_1} w_{k_1,k}^{(1)} \varphi_{k_1}^{(0)} \right), \quad k = 1, 2, \dots, K_2 \quad (3.4)$$

$$\varphi_k^{(0)} = \mathcal{S}_{\text{in}} \left(b_k^{(0)} + w_{0,k}^{(0)} t + w_{1,k}^{(0)} W + w_{2,k}^{(0)} R + w_{3,k}^{(0)} Q \right), \quad k = 1, 2, \dots, K_1 \quad (3.5)$$

for any input values (t, W, R, Q) . Equations (3.2)-(3.3)-(3.4)-(3.5) give an example of fully connected deep neural network with two hidden layers. The input layer (3.5) takes (t, x) as inputs are returns K_1 “neurons” $\varphi_k^{(0)}$, referring to nonlinear transforms of linear combinations of the inputs. The nonlinear transformation is performed by the activation function \mathcal{S}_{in} . Then, the first hidden layer (3.4) is obtained by a linear combination of the input neurons composed with the activation function \mathcal{S}_1 . In a similar manner, the second hidden layer (3.3) is obtained by a linear combination of the neurons (3.4) composed with the activation function \mathcal{S}_2 . Finally, the output layer (3.2) is obtained by a linear combination of the neurons (3.3) composed with the output activation function \mathcal{S}_{out} . We choose a sigmoid function $\mathcal{S}_{\text{out}}(x) = 1/(1 + e^{-x})$ for the output activation function, scaled by the factor $(W + P_t(W, Q))$ to enforce the consumption constraint (2.2). For the other activation functions, we choose Rectified Linear Unit (ReLU) activation functions $\mathcal{S}_{\text{in}}(x) = \mathcal{S}_1(x) = \mathcal{S}_2(x) = \max(0, x)$.

The set of parameters β contains all the weights $w^{(\ell)}$ and biases $b^{(\ell)}$, $\ell = 0, \dots, 3$

$$\beta = \left\{ \left(b_{k_1}^{(0)}, w_{k_0,k_1}^{(0)} \right)_{k_0=0,\dots,3}^{k_1=1,\dots,K_1}, \left(b_{k_2}^{(1)}, w_{k_1,k_2}^{(1)} \right)_{k_1=1,\dots,K_1}^{k_2=1,\dots,K_2}, \left(b_{k_3}^{(2)}, w_{k_2,k_3}^{(2)} \right)_{k_2=1,\dots,K_2}^{k_3=1,\dots,K_3}, \left(b_{k_3}^{(3)}, w_{k_3}^{(3)} \right)_{k_3=1,\dots,K_3} \right\}$$

In order to train the parameters (i.e. finding the optimal parameters β^* maximizing equation (3.1)), we perform a gradient descent using the Adam optimizer (Adaptive Moment Estimation, Kingma and Ba 2014), with parameter initialization of He et al. (2015), using the Python machine learning library PyTorch (Paszke et al., 2019), which takes care of gradient computations by automatic differentiation (Paszke et al., 2017).

In practice, we consider a global consumption DNN with two hidden layers as described by equations (3.2)-(3.3)-(3.4)-(3.5). There are four input dimensions (time t , wealth W , return R and inflation discount factor Q) and one output (consumption). We choose $K_1 = K_2 = 20$ neurons for the hidden layers, set the optimizer learning rate to 5×10^{-4} and the maximum number of iterations to 100,000. Finally, we produce independent training sets and testing sets containing $M = 100,000$ simulations using the ESG described in subsection 2.2. We perform our numerical tests on an Intel® CPU i7-7700 @ 3.60GHz* and NVIDIA® GPU GeForce® GTX 1070†, taking advantage of PyTorch’s built-in support for CUDA®‡.

The next section describes our numerical results.

*<https://ark.intel.com/content/www/us/en/ark/products/97128/intel-core-i7-7700-processor-8m-cache-up-to-4-20-ghz.html>

†<https://www.nvidia.com/en-us/geforce/10-series/>

‡<https://pytorch.org/docs/stable/notes/cuda.html>

4 Numerical results

In this section, we demonstrate numerical results from our trained DNN consumption policy, which estimates the optimal consumption taking into account age, gender, wealth, inflation, portfolio returns and the payments from means-tested Age Pension. In the numerical test, the individual is assumed to be aged 67 in year 2020, a single male homeowner with total wealth of A\$500,000 in account-based pension and no other testable assets or financial asset. He chooses the *Balanced* investment strategy, with 70% growth assets in domestic, international equities and property, and 30% in defensive assets in deposit, domestic and equity bonds as described in subsection 2.2.2. This person is entitled to the Australian mean-tested Age Pension. The maximum age is set to 108 years, so the total time horizon is 41 years.

We use our ESG to simulate $M = 100,000$ scenarios for each state variable to train our DNN optimal consumption policy. We simulate an independent testing set of M scenarios to compute the realized wealth trajectories, Age Pension eligibility and realized lifetime utility (equation (3.1)) from the trained DNN consumption policy. We compare the consumption policy from our DNN approach with other alternative draw-down strategies using the lifetime utility with risk aversion $\rho = 5$ and bequest motive $\phi = 0.5$. We also conduct sensitivity analysis for retirees who are less risk averse ($\rho = 2$), and those who have no bequest motive ($\phi = 0$). We also show how this policy performs with different initial starting wealth. Finally, we illustrate how the difference in mortality rates between males and females affect their respective optimal consumption policies.

4.1 Dynamic v.s. deterministic strategies

At time t , the trained DNN consumption policy estimates the optimal consumption level based on the available information from simulated inflation, portfolio returns, wealth and the Age Pension eligibility which depends on the wealth and compound inflation before time t . In Figure 1, we randomly pick one realization to demonstrate how our trained DNN policy works in the face of changes in inflation and portfolio returns. The upper subplot displays the simulated portfolio returns and inflation, while the lower subplot shows the consumption suggested by the DNN policy and the resulting wealth from the retirement age 67 to age 108.

The result shows that the optimal consumption at retirement age 67 is \$51,917 with partial Age Pension payment, the resulting wealth balance at age 68 is \$440,506 after being adjusted for inflation according to Eq. 2.7. At age 73 and 84, the huge drops in the market returns R_t have impact on the wealth and consumption at age 74 and 85. The consumption decreases over time as mortality rate increases. At age 107, the adjusted consumption is only \$22,900, that leads to a legacy wealth of \$85,929 at age 108. Note that after age 67, the wealth at time $t > 0$ also represents the legacy residual if this person die between t and $t + 1$.

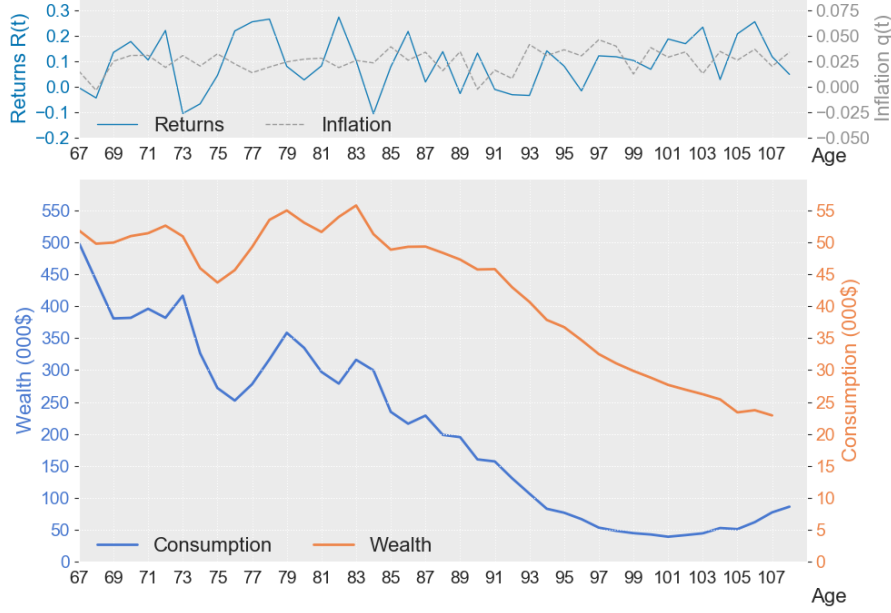


Figure 1: One realization of consumption and wealth under one simulated inflation and portfolio return with DNN optimal consumption policy.

4.2 Comparison with deterministic strategies

With the lifetime utility measure with risk aversion $\rho = 5$ and bequest motive $\theta = 0.5$, we compare our dynamic DNN consumption strategy with six alternative deterministic drawdown strategies discussed in [Chen et al. \(2020b\)](#) which are: (1) the mandated age-related *minimum* drawdown rules*; (2) 4% of the initial balance in real term ([Bengen, 1994](#)); (3) the Rule of Thumb (*RoT*), which is the minimum of the first digit of the age of the individual as the drawdown rate, plus 2% if the wealth is between A\$250,000 and A\$500,000 ([Bell, 2017](#); [De Ravin et al., 2019](#)); (4) the Association of Super Funds Australia’s (ASFA) *Modest* \$28,220 and (5) *Comfortable* \$44,183 lifestyle in June 2020; and (6) a *Luxury* consumption of \$50,000 per year.

We demonstrate such a comparison using one simulated path in [Figure 2](#). The realized lifetime utilities for this path under DNN, *RoT*, *minimum*, *modest*, 4%, *comfortable* and *luxury* drawdown strategies are: $U_{\text{DNN}} = -5.86 \times 10^4$, $U_{\text{RoT}} = -7.79 \times 10^4$, $U_{\text{min}} = -2.21 \times 10^5$, $U_{\text{mod}} = -5.01 \times 10^5$, $U_{\text{4pct}} = -1.24 \times 10^6$, $U_{\text{cmft}} = -2.5 \times 10^{55}$, $U_{\text{lux}} = -2.77 \times 10^{55}$ respectively. By definition, the realized lifetime utilities are negative, and the higher (i.e. the closer to zero) the better. For this particular scenario, the DNN strategy outperforms all the other strategies, yielding the highest lifetime utility. The *RoT* strategies, which is a simple rule developed under similar lifetime utility framework, takes the second place, followed by the mandated *minimum* and *modest* target drawdown strategies. Using 4% drawdown rule with an annual consumption of \$20,000 in real term, the remaining wealth keeps growing. It is not optimal as such a consumption level is so low that the accumulated wealth makes this person no longer eligible to receive any Age Pension payment after age 79 due to the asset test, and this person has to live solely on the 4% withdrawal from the account-based pension. The *comfortable* and *luxury* target consumption strategies are not sustainable under this utility measure, as the wealth runs out at age 106 and 96 respectively.

*The minimum withdrawal rate is available at: <https://www.ato.gov.au/rates/key-superannuation-rates-and-thresholds/?page=10>

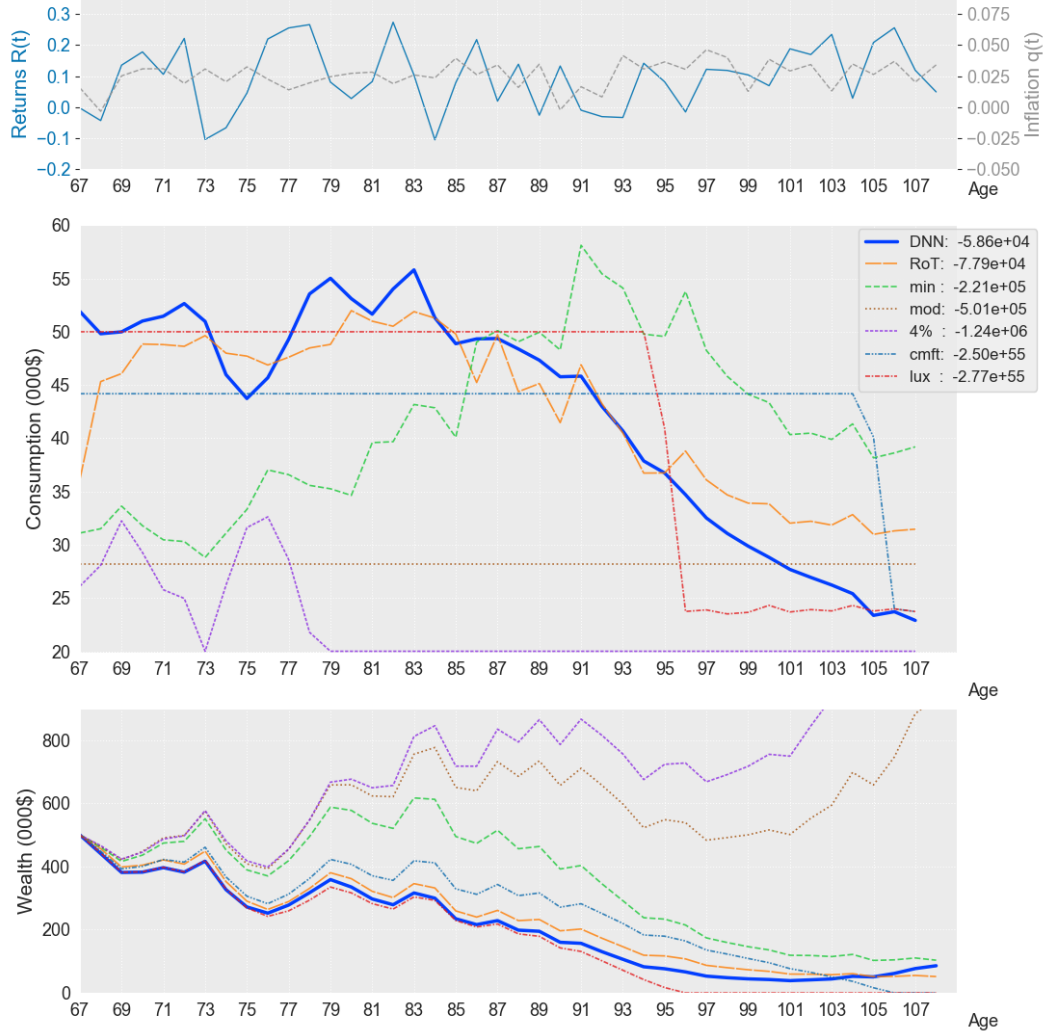


Figure 2: The simulated consumption and wealth paths under seven different drawdown strategies for one realisation of inflation and portfolio returns.

To investigate the utility differences across the 100,000 test simulations, we plot the kernel density estimate of the utility differences $U_{\text{DNN}} - U_i$ with $i \in \{\text{RoT}, \text{min}, \text{mod}, \text{cmft}, \text{4pct}, \text{lux}\}$ between the DNN policy and the six deterministic drawdown strategies in Fig 3. The horizontal axis of each subplot is log-scaled. The DNN policy performs better than all these strategies. The *RoT* strategy yields the least utility difference and performs relatively better than the rest of the five strategies.

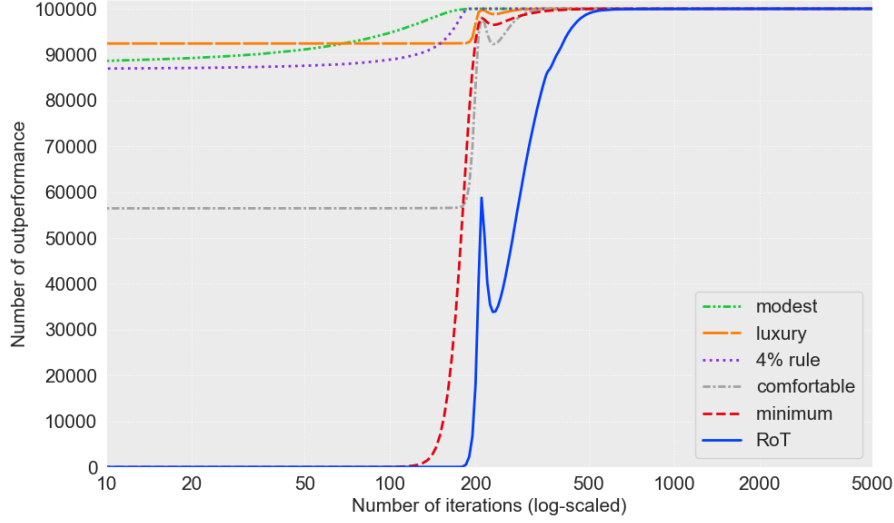


Figure 4: Number of DNN outperformance paths over the number of training iterations (in log-scale).

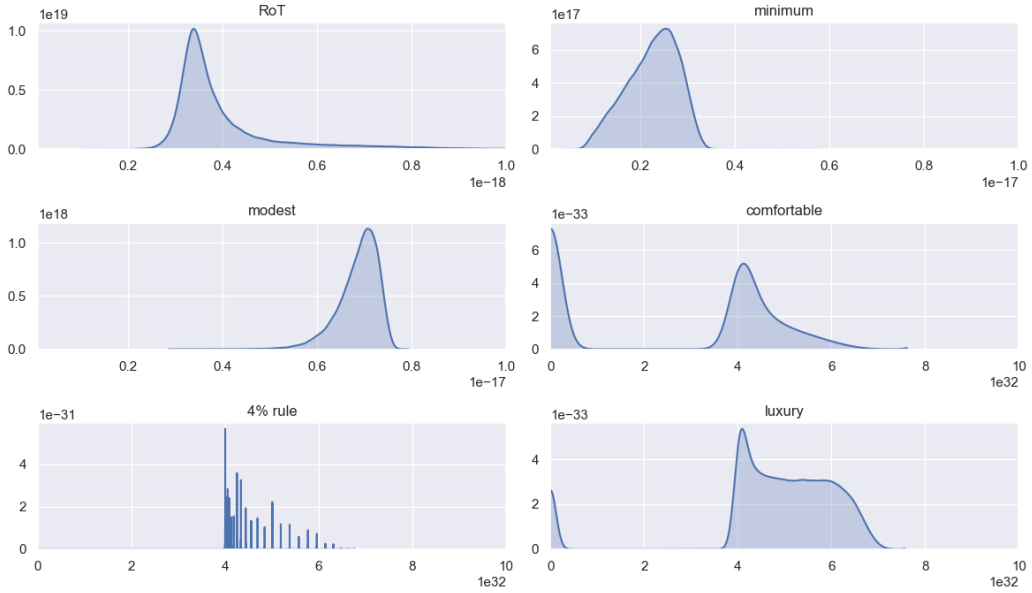


Figure 3: The kernel density estimate of the utility differences between the DNN drawdown and six deterministic drawdown strategies.

In addition, the performance of the DNN policy can also be determined with respect to the number of training iterations. In order to minimize the loss function (3.1), the DNN policy is trained on $M = 100,000$ Monte Carlo scenarios and 100,000 iterations. To show the relationship between the performance of the DNN policy and the number of training iterations, we plot on Figure 4 the total number of testing scenarios for which the DNN consumption policy outperforms alternative strategies versus the number of iterations. Starting with random weights, our trained DNN policy begins to outperform the *modest*, *luxury* and *4%* drawdown rules in more than 80% of the scenarios after a few iterations, and in more than 90% of the scenarios after 200 iterations (completed in 2 minutes) except for the *RoT* strategy. Eventually, after less than 1000 iterations (completed in 10 minutes), the trained DNN policy outperforms the other six strategies on all 100,000 testing paths.

4.3 Utility parameters sensitivity

In this utility maximisation problem (2.1), the optimal policy also depends on the choice of utility parameters. We compare the differences in median consumption and median wealth between two consumption risk aversions ρ and two bequest motives ϕ for a male retiree. We use $\rho = 5$ and $\phi = 0.5$ as our base case, and conduct two analyses with lower risk aversion parameter $\rho = 2$ reported in Figure 5, and a lower bequest motive $\phi = 0$ reported in Figure 6. From the upper subplot of Figure 5, we can see that under lower risk aversion $\rho = 2$, the median of the first year optimal annual consumption (dashed orange curve) can start from a higher level of \$59,270, compared to \$51,910 for higher risk aversion $\rho = 5$ (solid orange curve). The lower subplot of Figure 5, shows that the consumption gap decreases first and changes of sign after age 87. To sum up, retirees with higher consumption risk aversion tend to save more for later consumption to avoid potential shortfalls, and their consumption curve is flatter.

The upper subplot of Figure 6 shows the median consumption and median wealth with ($\phi = 0.5$) and without ($\phi = 0$) bequest motive. Without any bequest motive, the medians of initial consumption c_0 is \$52,247, which is \$336 more than the optimal consumption \$51,910 with bequest motive. The lower subplot of Figure 6 shows that there is no significant difference in consumption until age 102 when the person can start to spend more if no desire to leave any legacy. Such results may be counter-intuitive, as one might think that a lot more can be spent in early retirement. However, our results indicate that even without any bequest motive, overspending at early retirement is not optimal. The reason is that capital returns play a very important role in the wealth aggregation in retirement as there is a tradeoff between consumption level and sustainability of the wealth. Therefore, the optimal consumption is less sensitive to the bequest motive parameter than to the risk aversion parameter.

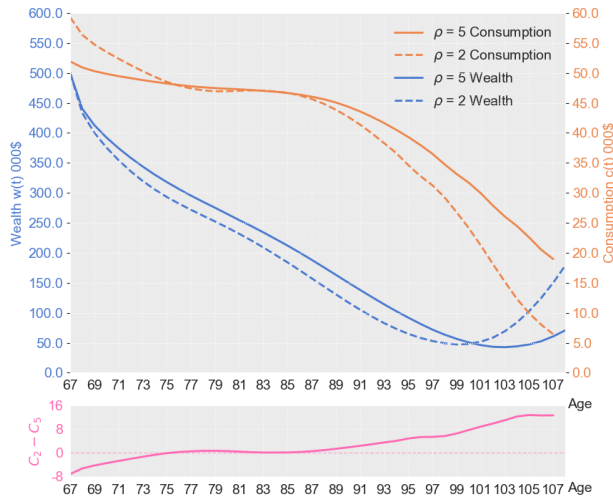


Figure 5: Comparison of the median consumption and median wealth with risk aversion parameter $\rho = 5$ and $\rho = 2$, with bequest motive $\phi = 0.5$, and the consumption difference over a retiree's lifetime.

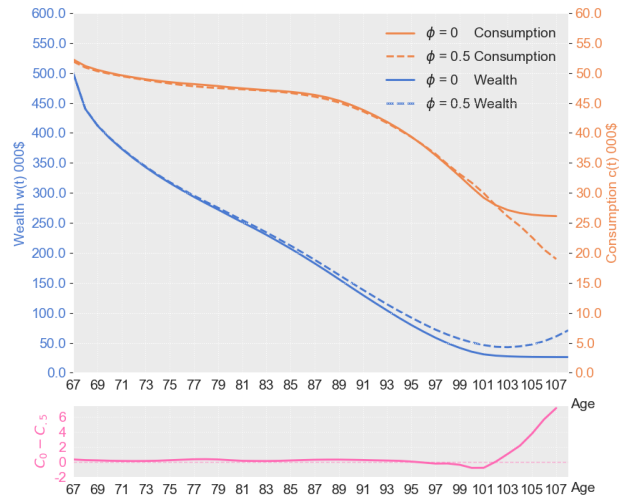


Figure 6: Comparison of the median consumption and median wealth with $\phi = 0.5$ and without $\phi = 0$ bequest motive, with risk aversion $\rho = 5$, and the consumption difference over a retiree's lifetime.

4.4 Consumption with different initial balances

We now investigate the effect of the initial wealth balance. We demonstrate the medians of the simulated wealth and consumption with starting balances of \$300,000, \$500,000, \$1,000,000 in Fig 7 and the consumption rates (consumption divided by wealth) in Fig 8. Because of the eligibility to receive full or partial Age Pension from the government for the retirees who own asset below the asset test limit, the retirement consumption is not proportional to the initial wealth. Retirees with lower wealth can draw down at a higher rate as there exist a pension *safety net*.

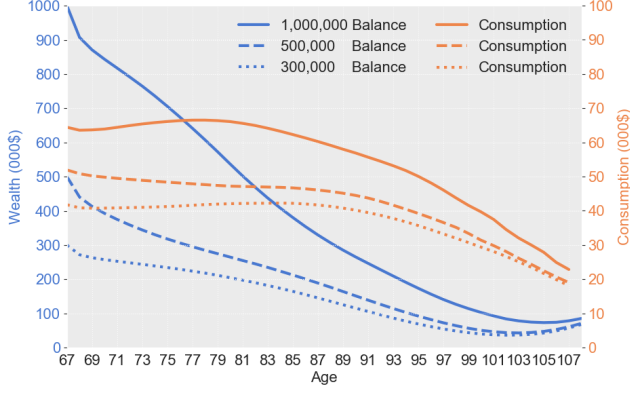


Figure 7: Comparison of the wealth and consumption over a retiree’s lifetime with different initial wealth w_0 .

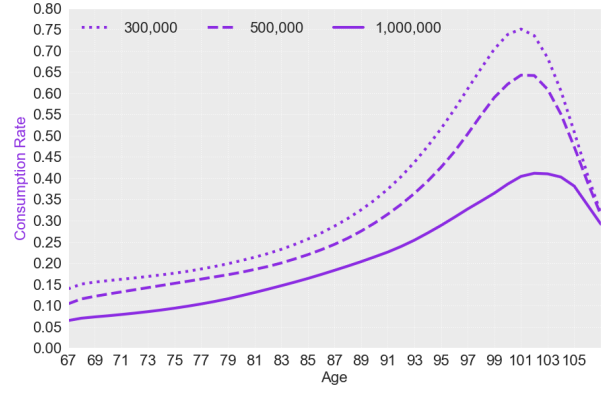


Figure 8: Comparison of the consumption rate over a retiree’s lifetime with different initial wealth w_0 .

4.5 Gender difference in consumption

Finally, we investigate the effect of gender on optimal consumption decisions during retirement. The Life Table 2015-2017 from ABS shows that the mortality of males is higher than that of females. In 2020, the life expectancy with 25 year improvement factor for age 65 is 85.5 for male and 87.9 for female (Australian Government Actuary, 2017). To obtain realistic measure of longevity, we consider the possible future improvements in mortality that may occur in the future. We implement the adjustment for mortality with the 25 year improvement factor[†] to project the mortality that could be expected to occur over a retiree’s lifetime.

In Figure 9, we plot the median of the simulated optimal consumption controlled by the DNN policy and the resulting wealth for a male and a female aged 67 with initial balance $w_0 = 500,000$. From Figure 9, we can observe a small effect of gender on consumption decisions: we can see that for a 67-year-old man and woman retiring with the same initial wealth, it is optimal for the man to spend more than the women until age 84 either with or without any bequest motive. Males have higher mortality rate and thus less longevity risk than females, and therefore it is optimal for them to consume slightly more in early retirement age. Conversely, women have greater longevity risk and therefore should consume slightly more conservatively than men in early retirement. Such lifetime uncertainty increases consumption impatience which is consistent with the findings in Huang et al. (2012) and Irving Fisher’s impatience theory (Fisher, 1930) in behavioral economics.

5 Conclusion

In this paper, we propose a deep neural network (DNN) optimal consumption policy analysis for the decumulation phase in a defined contribution (DC) pension system under a lifetime utility framework. The trained DNN can estimate the optimal consumption level for a retiree under any financial conditions that could happen during retirement. This DNN approach is independent of the simulation tool used to represent the possible future economic conditions. In practice, we propose and use a specific seven-factor Economic Scenario Generator (ESG), sufficient for decumulation analysis, and calibrate it to Australian market data.

We demonstrate that a DNN-based decumulation policy can successfully be trained from a realistic multivariate economic scenario generator in a matter of minutes. Our numerical tests demonstrate that the DNN-based policy outperforms six common deterministic decumulation rules by yielding higher lifetime utility for all testing scenarios after less than 1000 training iterations (completed in 10 minutes). We also report the densities of lifetime utility improvement provided by the DNN consumption policy compared to these deterministic policies. A sensitivity analysis with respect to the risk aversion parameter ρ reveals that a higher consumption risk aversion generates a smoother and flatter consumption pattern, with less variation over time. This contrasts with the bequest motive parameter ϕ , which is shown to have a negligible effect

[†]Details about the mortality improvement factors can be found on the Australian Government Actuary website: http://www.ag.gov.au/publications/life_table_2015-17/default.asp

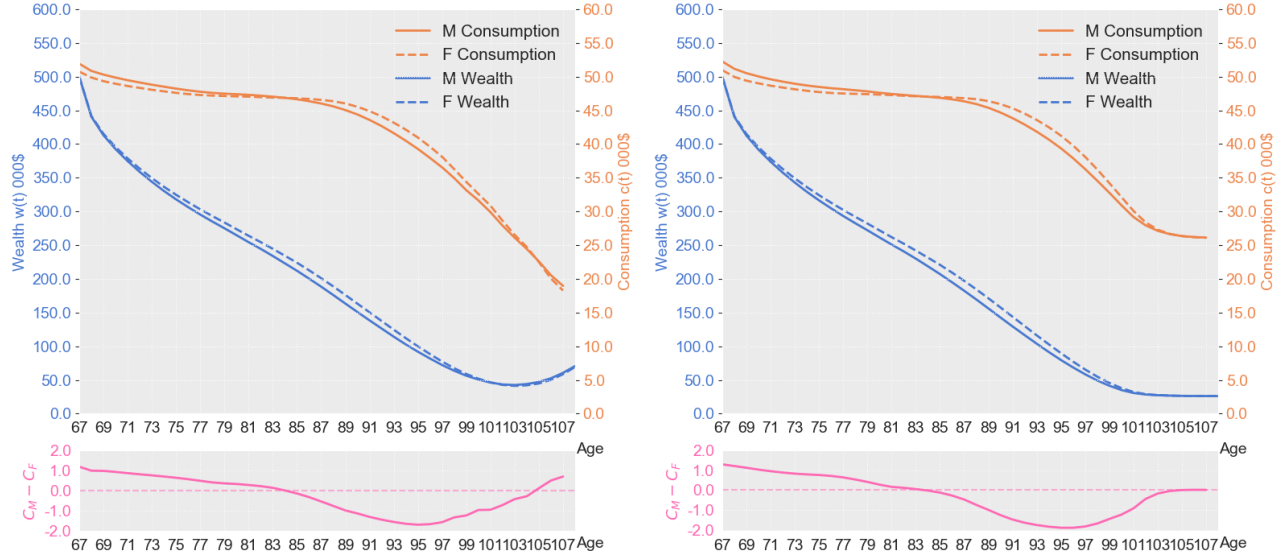


Figure 9: Comparison of the median consumption and median wealth between a male and a female with ($\phi = 0.5$, left) and without ($\phi = 0$, right) bequest motive under consumption risk aversion $\rho = 5$.

on optimal consumption until very late in retirement. Due to the cushion provided by the means-tested Age Pension payment, we observe that the optimal consumption is not proportional to the wealth of the retiree. Finally, gender has a small effect on optimal consumption due to the difference in mortality between males and females. Our results suggest that females should consume slightly less in early retirement (before age 84) to mitigate their greater longevity risk.

The DNN-policy approach developed in this paper for Australia can be applied to similar DC systems in other countries (e.g. UK DC system, USA 401(k)) with the necessary country adjustments and taking into account the government funded pension payment policy. Moreover, it can be extended to incorporate other financial decisions such as asset allocation or partial annuitisation, which we leave for future research.

References

- Ahlgrim, K. C., D’Arcy, S. P., and Gorvett, R. W. (2005). Modeling financial scenarios: A framework for the actuarial profession. *Proceedings of the Casualty Actuarial Society*, 92(177):177–238.
- Andréasson, J., Shevchenko, P., and Novikov, A. (2017). Optimal consumption, investment and housing with means-tested public pension in retirement. *Insurance: Mathematics and Economics*, 75:32–47.
- Australian Government Actuary (2017). Australian life table 2015-2017. Technical report, Australian Government Actuary. Available at http://www.aga.gov.au/publications/life_table_2015-17/default.asp.
- Bachouch, A., Huré, C., Langrené, N., and Pham, H. (2018). Deep neural networks algorithms for stochastic control problems on finite horizon: numerical applications. arXiv:1812.05916.
- Becker, S., Cheridito, P., and Jentzen, A. (2019). Deep optimal stopping. *Journal of Machine Learning Research*, 20:1–25.
- Beckmann, M. (1968). *Dynamic Programming of Economic Decisions*, volume 9 of *Ökonometrie und Unternehmensforschung*. Springer.
- Bell, D. (2017). Introducing the member’s default utility function version 1 (mduf v1). *Investment Magazine*, 137.
- Bengen, W. P. (1994). Determining withdrawal rates using historical data. *Journal of Financial planning*, 7(4):171–180.

- Butt, A. and Deng, Z. (2012). Investment strategies in retirement: in the presence of a means-tested government pension. *Journal of Pension Economics & Finance*, 11(2):151–181.
- Butt, A., Khemka, G., and Strickland, L. (2018). How academic research can inform default superannuation fund design and individual financial decision-making. *Australasian Journal of Applied Finance*, (1):40–49.
- Cairns, A., Blake, D., and Dowd, K. (2006). Stochastic lifestyling: optimal dynamic asset allocation for defined contribution pension plans. *Journal of Economic Dynamic and Control*, 30(5):843–877.
- Chen, W., Koo, B., Wang, Y., O’Hare, C., Langrené, N., Toscas, P., and Zhu, Z. (2020a). Using stochastic economic scenario generators to analyse uncertain superannuation and retirement outcomes.
- Chen, W., Minney, A., Toscas, P., Koo, B., Zhu, Z., and Pantelous, A. A. (2020b). Personalised drawdown strategies and partial annuitisation to mitigate longevity risk. *Finance Research Letters*, page 101644.
- De Ravin, J., Liu, E., van Rooen, R., Scully, P., and Wu, S. (2019). Spend your decennial age: a rule of thumb for retirement. *Actuaries Summit*.
- Ding, J., Kingston, G., and Purcal, S. (2014). Dynamic asset allocation when bequests are luxury goods. *Journal of Economic Dynamics and Control*, 38:65–71.
- Fécamp, S., Mikael, J., and Warin, X. (2019). Risk management with machine-learning-based algorithms. arXiv:1902.05287.
- Fisher, I. (1930). *Theory of interest: as determined by impatience to spend income and opportunity to invest it*. Augustusm Kelly Publishers, Clifton.
- Forsyth, P., Vetzal, K., and Westmacott, G. (2019). Management of portfolio depletion risk through optimal life cycle asset allocation. *North American Actuarial Journal*, 23(3):447–468.
- Fry, E. (2019). Super funds look to AI to improve member engagement. *Investment Magazine*.
- Goodfellow, I., Bengio, Y., and Courville, A. (2016). *Deep learning*. Adaptive Computation and Machine Learning. The MIT Press.
- Guo, I., Langrené, N., Loeper, G., and Ning, W. (2019). Robust utility maximization under model uncertainty via a penalization approach. arXiv:1907.13345.
- Han, J. and E, W. (2016). Deep learning approximation for stochastic control problems. In *NIPS 2016, Deep Reinforcement Learning Workshop*.
- Han, J., Jentzen, A., and Weinan, E. (2018). Solving high-dimensional partial differential equations using deep learning. *Proceedings of the National Academy of Sciences*, 115(34):8505–8510.
- He, K., Zhang, X., Ren, S., and Sun, J. (2015). Delving deep into rectifiers: surpassing human-level performance on ImageNet classification. In *2015 IEEE International Conference on Computer Vision (ICCV)*, pages 1026–1034.
- Huang, H., Milevsky, M., and Salisbury, T. (2012). Optimal retirement consumption with a stochastic force of mortality. *Insurance: Mathematics and Economics*, 51(2):282–291.
- Huré, C., Pham, H., Bachouch, A., and Langrené, N. (2018). Deep neural networks algorithms for stochastic control problems on finite horizon: convergence analysis. arXiv:1812.04300.
- Jin, Z., Liu, G., and Yang, H. (2020). Optimal consumption and investment strategies with liquidity risk and lifetime uncertainty for Markov regime-switching jump diffusion models. *European Journal of Operational Research*, 280(3):1130–1143.
- Kingma, D. and Ba, J. (2014). Adam: a method for stochastic optimization. In *3rd International Conference for Learning Representations (ICLR)*.

- Li, Y. and Forsyth, P. A. (2019). A data-driven neural network approach to optimal asset allocation for target based defined contribution pension plans. *Insurance: Mathematics and Economics*, 86:189–204.
- Mao, H., Ostaszewski, K., and Wang, Y. (2014). Optimal retirement age, leisure and consumption. *Economic Modelling*, 43:458–464.
- Moudiki, T. and Planchet, F. (2016). Economic scenario generators. In *Modelling in Life Insurance—A Management Perspective*, pages 81–104. Springer.
- Paszke, A., Gross, S., Chintala, S., Chanan, G., Yang, E., DeVito, Z., Lin, Z., Desmaison, A., Antiga, L., and Lerer, A. (2017). Automatic differentiation in PyTorch.
- Paszke, A., Gross, S., Massa, F., Lerer, A., Bradbury, J., Chanan, G., Killeen, T., Lin, Z., Gimelshein, N., Antiga, L., Desmaison, A., Kopf, A., Yang, E., DeVito, Z., Raison, M., Tejani, A., Chilamkurthy, S., Steiner, B., Fang, L., Bai, J., and Chintala, S. (2019). PyTorch: an imperative style, high-performance deep learning library. In Wallach, H., Larochelle, H., Beygelzimer, A., d'Alché-Buc, F., Fox, E., and Garnett, R., editors, *Advances in Neural Information Processing Systems 32*, pages 8024–8035. Curran Associates, Inc.
- Poggio, T., Mhaskar, H., Rosasco, L., Miranda, B., and Liao, Q. (2017). Why and when can deep-but not shallow-networks avoid the curse of dimensionality: a review. *International Journal of Automation and Computing*, 14(5):503–519.
- Rust, J. (1996). Numerical dynamic programming in economics. *Handbook of computational economics*, 1:619–729.
- Şahin, Ş., Cairns, A., and Kleinow, T. (2008). Revisiting the Wilkie investment model. In *18th International AFIR Colloquium, Rome*.
- Sneddon, T., Reeson, A., Zhu, Z., Stephenson, A., Hobman, E. V., Toscas, P., et al. (2016). Superannuation drawdown behaviour. *JASSA*, (2):42.
- Sutton, R. and Barto, A. (2018). *Reinforcement Learning - An Introduction*. Adaptive Computation and Machine Learning. The MIT Press, 2nd edition.
- Thorp, S., Kingston, G., and Bateman, H. (2007). Financial engineering for australian annuitants. *Retirement Provision in Scary Markets*, page 123.
- Towers Watson (2020). Global pension fund assets edge upwards. Technical report.
- Wilkie, A. D. (1984). A stochastic investment model for actuarial use. *Transactions of the Faculty of Actuaries*, 39:341–403.
- Wilkie, A. D. (1995). More on a stochastic asset model for actuarial use. *British Actuarial Journal*, 1(5):777–964.
- Wilkie, A. D. and Şahin, Ş. (2017). Yet More on a Stochastic Economic Model: Part 3B: Stochastic Bridging for Retail Prices and Wages. *Annals of Actuarial Science*, 11(1):100–127.
- Wilkie, A. D. and Şahin, Ş. (2019). Yet More on a Stochastic Economic Model: Part 5: a Vector Autoregressive (VAR) Model for Retail Prices and Wages. *Annals of Actuarial Science*, 13(1):92–108.
- Yaari, M. E. (1964). On the consumer’s lifetime allocation process. *International Economic Review*, 5(3):304–317.
- Yaari, M. E. (1965). Uncertain lifetime, life insurance, and the theory of the consumer. *The Review of Economic Studies*, 32(2):137–150.
- Zhang, S., Hardy, M., and Saunders, D. (2018). Updating wilkie’s economic scenario generator for us applications. *North American Actuarial Journal*, 22(4):600–622.

Year	CPI(t)	$s(t)$ %	$E(t)$	$N(t)$	$B(t)$	$O(t)$	HPI(t)
1992	59.7	6.42	5808.3	902.2	1692.5	299.6	28.73
1993	60.8	5.25	6291.6	1602.4	1928.3	373.1	29.50
1994	61.9	5.47	7252.1	1591.3	1906.5	357.9	30.49
1995	64.7	7.57	7756.2	1817.0	2133.0	438.2	30.90
1996	66.7	7.59	8866.4	1937.9	2334.6	396.1	31.23
1997	66.9	5.28	11313.3	2491.4	2725.8	548.8	32.11
1998	67.4	5.32	11542.2	3541.8	3022.4	545.5	34.89
1999	68.1	4.93	13251.6	3830.8	3121.7	531.5	36.92
2000	70.2	6.23	15628.0	4742.7	3314.3	604.5	40.50
2001	74.5	4.97	17044.8	4457.9	3559.7	592.3	43.82
2002	76.6	5.07	16245.3	3410.4	3781.3	714.1	52.1
2003	78.6	4.67	15966.7	2778.2	4151.3	696.6	61.2
2004	80.6	5.49	19416.7	3316.6	4247.9	712.2	70.9
2005	82.6	5.66	24533.9	3318.6	4578.8	641.5	71.0
2006	85.9	5.96	30405.1	3978.3	4735.1	712.2	73.8
2007	87.7	6.42	39119.1	4287.3	4923.0	641.5	80.9
2008	91.6	7.81	33875.3	3375.9	5141.6	663.5	91.8
2009	92.9	3.25	27053.6	2827.8	5698.0	819.1	86.8
2010	95.8	4.89	30610.0	2975.3	6145.6	807.7	103.1
2011	99.2	4.99	34200.7	3054.4	6486.5	704.4	103.2
2012	100.4	3.49	31904.5	3039.0	7290.8	755.4	99.7
2013	102.8	2.80	39163.3	4045.1	7492.6	807.9	103.1
2014	105.9	2.70	45991.2	4870.5	7950.1	837.1	114.4
2015	107.5	2.15	48602.3	4686.0	8397.5	935.2	123.0
2016	108.6	1.99	48872.4	4557.9	8986.8	1074.1	132.1
2017	110.7	1.72	55758.6	5386.9	9009.23	999.5	147.3
2018	113.5	2.07	63015.4	5987.6	9287.2	1057.4	150.6
2019	114.8	1.29	70291.8	6636.4	10176.2	1174.3	138.1
2020	116.6	0.102	64116.9	6583.0	10601.6	1262.5	150.3

Table A.1: Australian historical data from June 1992 to June 2020.

A Calibration of ESG parameters

This Appendix details the historical data used to calibrate the ESG and provides the calibrated parameter values in order to make our results replicable. The ESG parameters are calibrated by ordinary least squares method using historical data from 1992, the year when the compulsory contribution system started, to 2020 as shown in Table A.1. The short-term interest rates $s(t)$ are the 90-day bank accepted bills from the RBA website. Most data are indices, except for the short-term interest rates $s(t)$, therefore we first compute the returns using the log-ratio of two consecutive indices in time. The inflation rate $q(t) = \log(\text{CPI}(t)/\text{CPI}(t-1))$ is the log-ratio of the all groups Consumer Prices Index CPI(t) from the RBA. The domestic $e(t)$ and international equity total returns $n(t)$ are computed from the S&P/ASX200 Accumulation Index $E(t)$ and MSCI World ex-Australia Net Index (in Australian Dollar) $N(t)$ respectively. While the domestic $b(t)$ and international bond returns $o(t)$ are computed from the AusBond Index $B(t)$ and Citigroup World Government Bond Index $O(t)$. These four indices are from the Bloomberg terminal. The house price growth $h(t)$ comes from the House Price Index HPI(t) which is the Established House Price Index (weighted average of 8 capital cities) from the ABS website*.

We assume that the residuals are conditionally independent. Figure 10 shows the lower triangular part of their correlation matrix which exhibit low correlations as expected.

*The ABS has compiled a House Price Index (HPI) since 1986. A significant review of the HPI occurred in 2004 and a new series of HPI was introduced in 2005. We scaled the HPI before 2005 to keep the house price returns consistent with the data before 2005. More details about the HPI is available at <https://www.abs.gov.au/ausstats/abs@.nsf/mf/6416.0>.

Variable dynamics	Params	Values
1, Price inflation $q(t)$	μ_q	0.024
$q(t) = (1 - \phi_q)\mu_q + \phi_q q(t-1) + \epsilon_q(t)$	ϕ_q	0.1346
	σ_q	0.012
2, Short-term interest rate $s(t)$	μ_S	0.141
$S(t) = \phi_S S(t-1) + (1 - \phi_S)(\mu_S - \mu_q) + \epsilon_s(t)$	ϕ_S	0.813
$s(t) = S(t) + q(t)$	σ_S	0.015
3, Domestic equity returns $e(t)$	μ_e	0.085
$e(t) = \phi_e e(t-1) + (1 - \phi_e)\mu_e + \epsilon_e$	ϕ_e	0.164
	σ_e	0.119
4, International equity returns $n(t)$	$\psi_{n,0}$	-0.018
$n(t) = \psi_{n,0} + \psi_{n,1}n(t-1) + \psi_{n,2}e(t) + \epsilon_n(t)$	$\psi_{n,1}$	0.104
	$\psi_{n,2}$	0.911
	σ_n	0.090
5, Domestic bond $b(t)$	$\psi_{b,0}$	0.073
	$\psi_{b,1}$	-0.103
$b(t) = \psi_{b,0} + \psi_{b,1}b(t-1) + \psi_{b,2}n(t) + \epsilon_b(t)$	$\psi_{b,2}$	-0.050
	σ_b	0.036
6, International bond $o(t)$	$\psi_{o,0}$	-0.026
	$\psi_{o,1}$	1.340
$o(t) = \psi_{o,0} + \psi_{o,1}e(t) + \psi_{o,2}n(t) + \epsilon_o(t)$	$\psi_{o,2}$	-0.200
	σ_o	0.081
7, House price $h(t)$	$\psi_{h,0}$	0.066
	$\psi_{h,1}$	-0.489
$h(t) = \psi_{h,0} + \psi_{h,1}q(t) + \psi_{h,2}b(t) + \epsilon_h(t)$	$\psi_{h,2}$	1.037
	σ_h	0.061

Table A.2: Dynamics of the variables and calibrated parameters of the ESG.

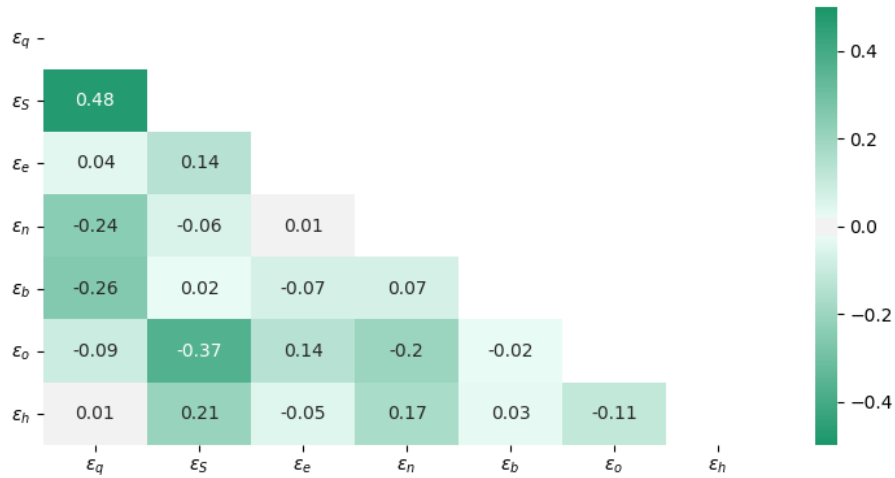


Figure 10: Cross-correlation matrix of the residuals.

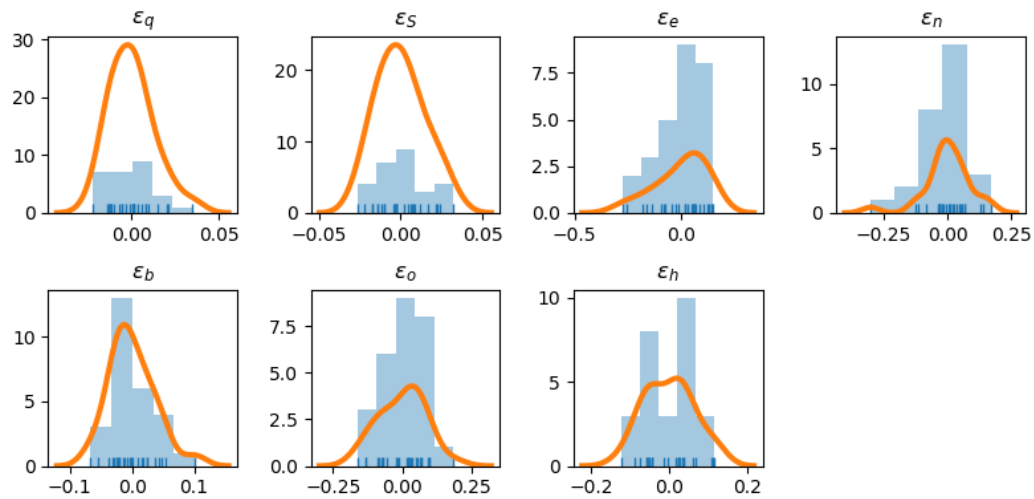


Figure 11: Kernel density estimate of empirical errors.

We plot the histogram and the kernel density estimate of the empirical errors. The empirical distributions of the residuals look not too far from being centered, unimodal, symmetric, and can be approximated by normal variables.